

Layered Perovskite Oxychloride $\text{Bi}_4\text{NbO}_8\text{Cl}$: A Stable Visible Light Responsive Photocatalyst for Water Splitting

Hironori Fujito,^{†,‡} Hironobu Kunioku,^{†,‡} Daichi Kato,[†] Hajime Suzuki,[†] Masanobu Higashi,[†] Hiroshi Kageyama,^{*,†,§} and Ryu Abe^{*,†,§}

[†]Department of Energy and Hydrocarbon Chemistry, Graduate School of Engineering, Kyoto University, Nishikyo-ku, Kyoto 615-8510, Japan

[§]CREST, Japan Science and Technology Agency (JST), Kawaguchi, Saitama 332-0012, Japan

S Supporting Information

ABSTRACT: Mixed anion compounds are expected to be a photocatalyst for visible light-induced water splitting, but the available materials have been almost limited to oxynitrides. Here, we show that an oxychloride $\text{Bi}_4\text{NbO}_8\text{Cl}$, a single layer Sillen–Aurivillius perovskite, is a stable and efficient O_2 -evolving photocatalyst under visible light, enabling a Z-scheme overall water splitting by coupling with a H_2 -evolving photocatalyst (Rh-doped SrTiO_3). It is found that the valence band maximum of $\text{Bi}_4\text{NbO}_8\text{Cl}$ is unusually high owing to highly dispersive O-2p orbitals (not Cl-3p orbitals), affording the narrow band gap and possibly the stability against water oxidation. This study suggests that a family of Sillen–Aurivillius perovskite oxyhalides is a promising system to allow a versatile band level tuning for establishing efficient and stable water-splitting under visible light.

Developing stable photocatalyst materials that can efficiently split water under visible light is of great technical challenge.¹ Over the past decade, metal oxynitride semiconductor materials have been extensively explored for such photocatalysts.¹ Although a number of oxynitrides such as TaON , BaTaO_2N , SrNbO_2N , and LaTiO_2N exhibit photoelectrochemical water splitting,² there are so far only a few oxynitrides (e.g., $(\text{Ga}_{1-x}\text{Zn}_x)(\text{N}_{1-x}\text{O}_x)$ and $\text{LaMg}_{1/3}\text{Ta}_{2/3}\text{O}_2\text{N}$) that show photocatalytic water splitting.³ In addition, these oxynitrides are mostly unstable upon light irradiation; appropriate surface modifications are required to suppress the competitive oxidation of N^{3-} by photogenerated holes.^{2,3c,d}

Other mixed anion compounds such as oxysulfides⁴ and oxyhalides⁵ are considered as potential photocatalysts for visible light-induced water splitting, because the lower electronegativity of S and X (X = Cl, Br, I) locates S-3p, Cl-3p, Br-4p, or I-5p orbitals at higher energies than O-2p orbitals, resulting in a reduction of the band gap relative to corresponding oxides. For example, the band gap of BiOX decreases markedly from 3.48 eV in BiOCl, to 2.93 eV in BiOBr, and to 1.91 eV in BiOI, accompanied by negative shift of valence band maximum (VBM),⁶ in accordance with the reduced electronegativity (Cl > Br > I). Although BiOCl is capable of oxidizing water to O_2 in the presence of sacrificial electron-acceptor Ag^+ under UV irradiation,⁷ neither O_2 nor H_2 evolution has been achieved under visible light on such

oxyhalides. An oxysulfide $\text{Sm}_2\text{Ti}_2\text{S}_2\text{O}_5$ (band gap: ~ 2.0 eV) is known as a H_2 -evolving photocatalyst in Z-scheme water splitting systems, but UV light irradiation is necessary to excite the O_2 -evolving photocatalyst, rutile- TiO_2 .⁸ Unfortunately, other than oxynitrides,³ stable photocatalytic water splitting under visible light has not been reported in mixed anion compounds (even through Z-scheme with redox), despite the expected reduced band gap. Facile self-oxidation of nonoxide anions by photogenerated holes at valence band near VBM may be an essential problem.

$\text{Bi}_4\text{MO}_8\text{Cl}$ (M = Nb, Ta) is a Sillen–Aurivillius perovskite phase consisting of single-layer MO_4 perovskite blocks that are separated by $(\text{Bi}_2\text{O}_2)_2\text{Cl}$ blocks (Figure 1a).⁹ Recently,

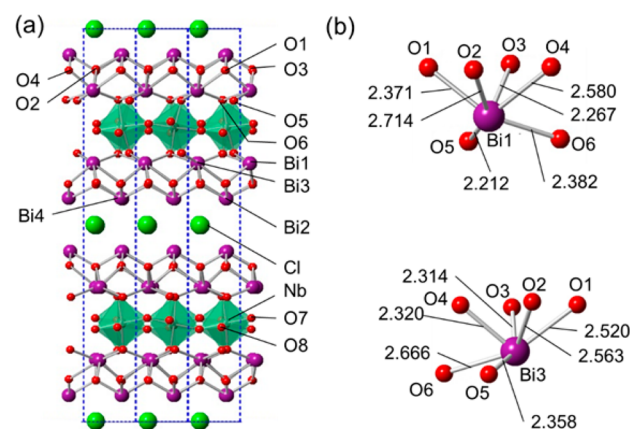


Figure 1. (a) Crystal structure of $\text{Bi}_4\text{NbO}_8\text{Cl}$, comprehensively expressed as $(\text{Bi}_2\text{O}_2)_2\text{ClNbO}_4$. (b) Coordination environment around Bi1 and Bi3 with Bi–O bond lengths (in Å).

photocatalytic activity by dye degradation (but not water splitting) was found in $\text{Bi}_4\text{MO}_8\text{Cl}$.¹⁰ Here, we recognized two remarkable features in these oxychlorides. The first is the size of band gaps (2.4 eV for Nb)¹⁰ being much narrower than those of other oxychlorides such as BiOCl (3.4 eV).⁵ The second is a reverse trend of absorption edge between $\text{Bi}_4\text{MO}_8\text{Cl}$ and isostructural $\text{Bi}_4\text{MO}_8\text{Br}$ (502 and 488 nm for Ta).¹¹ However, the origin of these features has not been verified.

Received: October 26, 2015

Published: February 15, 2016

Here, we demonstrate that $\text{Bi}_4\text{NbO}_8\text{Cl}$ is a stable and efficient oxygen evolution photocatalyst and exhibits visible light-induced overall water splitting through the Z-scheme mechanism. From experimental and theoretical results, the VBM is found to be unusually high (vs typical oxides and oxychlorides) as a result of highly dispersive O-2p orbitals in the valence band. This suggests sizable interactions within and between Bi–O and Nb–O slabs, offering a potential of extensive band engineering in a general family of Sillen–Aurivillius perovskite compounds.

$\text{Bi}_4\text{NbO}_8\text{Cl}$ (particle size of $\sim 5 \mu\text{m}$, see Figure S1 for a SEM image) was prepared by a solid-state reaction. Stoichiometric quantities of Bi_2O_3 (Wako, 99.99%), BiOCl (Wako, 99.5%) and Nb_2O_5 powders (Kojundo Chemicals, 99.9%) were weighed, mixed, and heated in an evacuated silica tube at 1173 K for 20 h.⁹ For comparison, $\text{Bi}_4\text{NbO}_8\text{Br}$ was synthesized in a similar manner using BiOBr . BiOBr was prepared by a soft liquid deposition method.¹² Powder X-ray diffraction showed that both compounds are of single phase (Figure S2). Detailed experimental conditions are given in Supporting Information (SI).

UV–vis diffuse reflectance spectrum of $\text{Bi}_4\text{NbO}_8\text{Cl}$ exhibited the absorption edge at 498 nm, which is obviously longer than 485 nm in $\text{Bi}_4\text{NbO}_8\text{Br}$ (Figure 2), in agreement with the

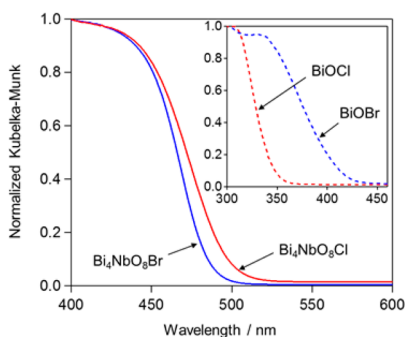


Figure 2. UV–vis diffuse reflectance spectra of $\text{Bi}_4\text{NbO}_8\text{Cl}$ and $\text{Bi}_4\text{NbO}_8\text{Br}$. For comparison, spectra of BiOCl and BiOBr are shown in the inset.

previous literatures,^{10,13} though our values appear to be slightly shorter. The flat-band potential of $\text{Bi}_4\text{NbO}_8\text{Cl}$ was determined from the Mott–Schottky plots in an aqueous Na_2SO_4 solution (pH = 2) (Figure S3). We obtained -0.48 V (vs Ag/AgCl) corresponding to -0.28 V (vs SHE at pH = 2). Supposing that the flat-band potential is located just below conduction band minimum (CBM), the VBM was estimated to be $\sim 2.11 \text{ V}$ using its band gap. The estimated VBM of $\text{Bi}_4\text{NbO}_8\text{Cl}$ is surprisingly high and affords higher CBM than the water reduction potential. For comparison, the same measurements were conducted for BiOCl , providing the absorption edge at 344 nm, the flat-band potential of -0.63 V (vs Ag/AgCl) corresponding to -0.43 V (vs SHE at pH = 2) and the VBM of $\sim 2.99 \text{ V}$ (Figure 3), in excellent agreement with previous results.¹³ Proposed band structures of $\text{Bi}_4\text{NbO}_8\text{Cl}$ and BiOCl are represented in Figure 3.

$\text{Bi}_4\text{NbO}_8\text{Cl}$ showed activity for H_2 evolution from an aqueous methanol solution (Figure S4). At present, the rate is quite low ($\sim 0.1 \mu\text{mol h}^{-1}$), but the steady H_2 evolution observed validates the above estimated CBM, which is slightly higher than the water reduction potential. On the other hand, a steady and high activity for O_2 evolution is recognized when

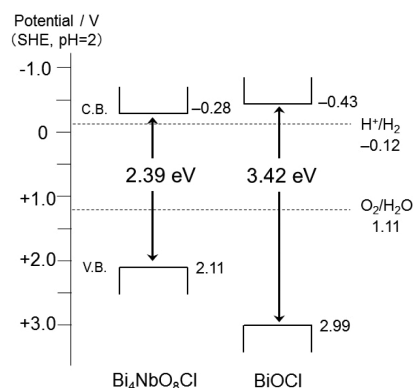


Figure 3. Proposed band structures of $\text{Bi}_4\text{NbO}_8\text{Cl}$ and BiOCl at pH = 2.0.

appropriate electron acceptors are used. As shown in Figure 4a, O_2 was generated with relatively steady rates under visible light

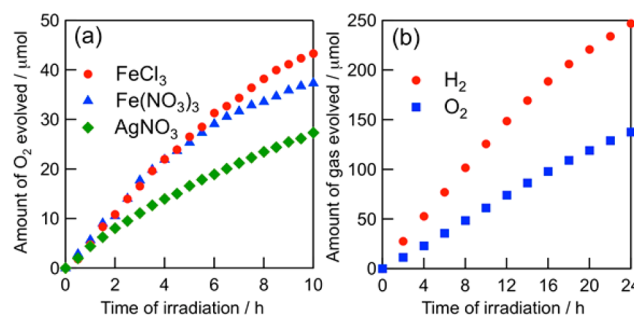


Figure 4. (a) Time courses of photocatalytic O_2 evolution under visible light on $\text{Bi}_4\text{NbO}_8\text{Cl}$ in the presence of various electron acceptors. (b) Time course of Z-scheme water splitting coupled with $\text{Ru}/\text{SrTiO}_3:\text{Rh}$ photocatalyst via $\text{Fe}^{3+}/\text{Fe}^{2+}$ redox mediator.

irradiation, from $\text{FeCl}_3(\text{aq})$, $\text{Fe}(\text{NO}_3)_3(\text{aq})$, and $\text{AgNO}_3(\text{aq})$. Although a slight reduction in O_2 generation rate is appreciable, such a behavior is generally observed even for other conventional photocatalysts such as WO_3 and BiVO_4 during the half reaction, which has been interpreted as due to the light shielding by the deposited Ag metal particles or the occurrence of backward reaction (i.e., re-oxidation of Fe^{2+} by photo-generated holes) instead of water oxidation. For the Fe-based electron acceptors, we confirmed the generation of almost stoichiometric amounts of Fe^{2+} , while no change in the Cl component was observed in the XPS analysis (Table S1). As shown in Figures S1 and S5, no significant change in particle size (SEM images) and in Raman spectra of $\text{Bi}_4\text{NbO}_8\text{Cl}$ is observed. These results indicated clearly the photocatalytic water oxidation on $\text{Bi}_4\text{NbO}_8\text{Cl}$, accompanied by stoichiometric reduction of Fe^{3+} to Fe^{2+} . Note that $\text{Bi}_4\text{NbO}_8\text{Br}$ also generated O_2 in the presence of Fe^{3+} under visible light, though the rate was lower (Figure S6).

The apparent quantum efficiency for O_2 evolution on the $\text{Bi}_4\text{NbO}_8\text{Cl}$ was determined to be $\sim 0.4\%$ in 5 mM $\text{FeCl}_3(\text{aq})$ under the irradiation of monochromatic light at 420 nm ($\sim 25 \text{ mW}/\text{cm}^2$). This value is comparable to the reported values on the conventional O_2 -evolving photocatalysts such as unmodified WO_3 ($\sim 0.4\%$ at 405 nm)¹⁴ under the similar reaction condition (i.e., in 10 mM of $\text{FeCl}_3(\text{aq})$). We expect significant improvement in the apparent quantum efficiency by appro-

appropriate surface modifications¹⁵ and/or optimization of synthesis procedure of photocatalysts.

Most remarkably, as shown in Figure 4b, a simultaneous evolution of H₂ and O₂ under visible light was successfully observed for the Bi₄NbO₈Cl photocatalyst coupled with a H₂-evolving photocatalyst of Rh-doped SrTiO₃,¹⁶ through the Z-scheme mechanism involving a redox cycle of Fe³⁺/Fe²⁺.¹⁷ A slight decrease in gas evolution rate in the later period of reaction is probably due to the occurrence of other backward reactions on Ru metal cocatalyst, i.e., the catalytic formation of water from the evolved H₂ and O₂ and/or photocatalytic reduction of O₂, as often reported in other Z-scheme systems. A long-term reaction (for 60 h) with periodical evacuation of gas phase resulted in the generation of ~304.7 μmol of O₂ gas in total (Figure S7), sufficiently exceeding the molar amount of Bi₄NbO₈Cl (137 μmol) used for the reaction, indicating that this reaction proceeded photocatalytically.

In order to obtain insights into the origin of the highly up-shifted VBM in Bi₄NbO₈Cl, we conducted first-principles calculations for Bi₄NbO₈Cl and Bi₄NbO₈Br using the generalized gradient approximation of DFT using CASTEP (see SI) for detail.¹⁸ Figure S8 represents the calculated electronic band structure, while the total density of states (TDOS) and the partial density of states (PDOS) are shown in Figures 5 and S9. As expected, the Br-4p orbitals in Bi₄NbO₈Br

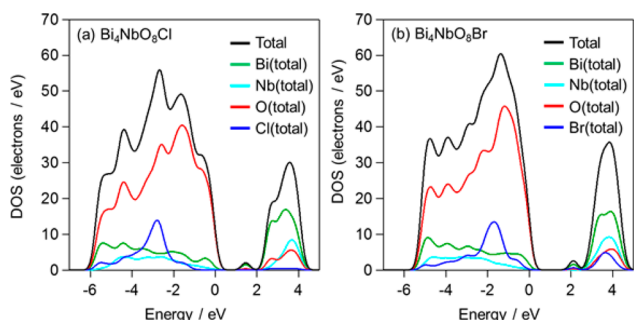


Figure 5. TDOS of (a) Bi₄NbO₈Cl and (b) Bi₄NbO₈Br, and PDOS projected onto each constituent element.

are located at a higher energy level than the Cl-3p orbitals in Bi₄NbO₈Cl. Quite unexpectedly, the VBM is predominantly composed of O-2p orbitals. The situation is in stark contrast to simple oxyhalides BiOCl and BiOBr, in which Cl-3p and Br-4p orbitals mainly contribute to the DOS near VBM (Figure S10).⁶ Each of the O-2p orbitals (O1–O8) in Bi₄NbO₈Cl possesses a large dispersion (Figure S9). Consistently, the bond valence sum (BVS) calculations for all oxygen sites gave reasonable values of –1.70 to –2.38 (Table S2). Since the outer Bi atoms (Bi1/Bi3) are bonded to the apical oxygen atoms (O5/O6) of the NbO₆ octahedral layer (Figure 1b), the highly dispersive nature of O-2p orbitals is likely to originate from fairly strong interactions within and between the Bi–O and Nb–O layers. Note that the (small) DOS at CBM is composed mainly of Bi-6p orbitals at Bi2/Bi4 (Figures 3 and S9).

The peculiar band structure of Bi₄NbO₈Cl seems to give an impact on the stability during photocatalytic activity. For mixed anion materials (oxynitrides, oxysulfides, and oxyhalides), in general, the DOS near VBM are composed mostly of p orbitals of nonoxide anion (S²⁻, N³⁻, X⁻) with a smaller electronegativity. Thus, photogenerated holes around VBM are prone

to self-oxidation during the photocatalytic (or photoelectrochemical) water oxidation. Namely, the photogenerated holes may preferentially oxidize these anions (e.g., 2N³⁻ + 6h⁺ → N₂, 2X⁻ + 2h⁺ → X₂) instead of water molecules, resulting in photocorrosion and/or photooxidation to give an inactive surface.¹⁹ On the contrary, the VBM of Bi₄NbO₈Cl is mainly composed of the dispersive O-2p band. Thus, we believe that the holes populated on the stable oxygen anions near VBM can efficiently oxidize water, without suffering from deactivation by self-oxidation of Cl⁻.

In summary, we showed that the layered oxychloride Bi₄NbO₈Cl with the Sillen–Aurivillius perovskite works as a stable photocatalyst for water oxidation under visible light. Other than oxynitrides, Bi₄NbO₈Cl has achieved overall water splitting under visible light irradiation (through the Z-scheme mechanism) for the first time among mixed anion compounds. The highly dispersive O-2p band extending to VBM not only allows the substantially negative VBM (and CBM) but also accounts for the stability against water oxidation under visible light. The present result strongly suggests that fine and extensive control of the valence and conduction band edge energies is possible by manipulating the perovskite block as well as the (Bi₂O₂)₂X block in the Sillen–Aurivillius phases, with a general formula of [(Bi₂O₂)₂X]³⁺[A_{n-1}B_nO_{3n+1}]³⁻ (n = 1, 2, 3, ...).²⁰ This will offer us a possibility to achieve more efficient water splitting by harvesting a wider range of solar light spectrum and, ultimately, overall water splitting using a single material.

■ ASSOCIATED CONTENT

📄 Supporting Information

The Supporting Information is available free of charge on the ACS Publications website at DOI: 10.1021/jacs.5b11191.

Experimental details and data (PDF)

■ AUTHOR INFORMATION

Corresponding Authors

*kage@scl.kyoto-u.ac.jp

*ryu-abe@scl.kyoto-u.ac.jp

Author Contributions

‡These authors contributed equally.

Notes

The authors declare no competing financial interest.

■ ACKNOWLEDGMENTS

This work was supported by the Core Research for Evolutional Science and Technology (CREST) from the Japan Science and Technology Agency (JST). We are grateful to Prof. Aron Walsh for helpful discussion. Computation time was provided by the SuperComputer System, Institute for Chemical Research, Kyoto University. The authors are also indebted to the technical division of Institute for Catalysis, Hokkaido University for their help in building the experimental equipment.

■ REFERENCES

- (1) (a) Esswein, M. J.; Nocera, D. G. *Chem. Rev.* **2007**, *107*, 4022. (b) Maeda, K.; Domen, K. *J. Phys. Chem. C* **2007**, *111*, 7851. (c) Osterloh, F. E. *Chem. Mater.* **2008**, *20*, 35. (d) Kudo, A.; Miseki, Y. *Chem. Soc. Rev.* **2009**, *38*, 253. (e) Abe, R. *J. Photochem. Photobiol. C* **2010**, *11*, 179.

- (2) (a) Abe, R.; Higashi, M.; Domen, K. *J. Am. Chem. Soc.* **2010**, *132*, 11828. (b) Higashi, M.; Domen, K.; Abe, R. *J. Am. Chem. Soc.* **2013**, *135*, 10238. (c) Maeda, K.; Higashi, M.; Siritanaratkul, B.; Abe, R.; Domen, K. *J. Am. Chem. Soc.* **2011**, *133*, 12334. (d) Minegishi, T.; Nishimura, N.; Kubota, J.; Domen, K. *Chem. Sci.* **2013**, *4*, 1120.
- (3) (a) Maeda, K.; Teramura, K.; Lu, D. L.; Takata, T.; Saito, N.; Inoue, Y.; Domen, K. *Nature* **2006**, *440*, 295. (b) Lee, Y.; Terashima, H.; Shimodaira, Y.; Teramura, K.; Hara, M.; Kobayashi, H.; Domen, K.; Yashima, M. *J. Phys. Chem. C* **2007**, *111*, 1042. (c) Pan, C. S.; Takata, T.; Nakabayashi, M.; Matsumoto, T.; Shibata, N.; Ikuhara, Y.; Domen, K. *Angew. Chem., Int. Ed.* **2015**, *54*, 2955. (d) Xu, J. S.; Pan, C. S.; Takata, T.; Domen, K. *Chem. Commun.* **2015**, *51*, 7191.
- (4) Ishikawa, A.; Takata, T.; Kondo, J. N.; Hara, M.; Kobayashi, H.; Domen, K. *J. Am. Chem. Soc.* **2002**, *124*, 13547.
- (5) Zhang, K. L.; Liu, C. M.; Huang, F. Q.; Zheng, C.; Wang, W. D. *Appl. Catal., B* **2006**, *68*, 125.
- (6) Xiao, X.; Liu, C.; Hu, R. P.; Zuo, X. X.; Nan, J. M.; Li, L. S.; Wang, L. S. *J. Mater. Chem.* **2012**, *22*, 22840.
- (7) Jiang, Z. Y.; Liu, Y. Y.; Jing, T.; Huang, B. B.; Wang, Z. Y.; Zhang, X. Y.; Qin, X. Y.; Dai, Y. *RSC Adv.* **2015**, *5*, 47261.
- (8) Zhao, W.; Maeda, K.; Zhang, F. X.; Hisatomi, T.; Domen, K. *Phys. Chem. Chem. Phys.* **2014**, *16*, 12051.
- (9) Kusainova, A. M.; Zhou, W. Z.; Irvine, J. T. S.; Lightfoot, P. J. *Solid State Chem.* **2002**, *166*, 148.
- (10) Lin, X. P.; Huang, T.; Huang, F. Q.; Wang, W. D.; Shi, J. L. *J. Mater. Chem.* **2007**, *17*, 2145.
- (11) Zhang, K. L.; Xie, Z. G.; Fan, J.; Hu, X. Y.; Wang, J. J. *J. Environ. Eng.* **2012**, *138*, 259.
- (12) He, Y.; Zhang, Y. H.; Huang, H. W.; Tian, N.; Guo, Y. X.; Luo, Y. *Colloids Surf., A* **2014**, *462*, 131.
- (13) Zhang, L.; Han, Z.; Wang, W.; Li, X.; Su, Y.; Jiang, D.; Lei, X.; Sun, S. *Chem. - Eur. J.* **2015**, *21*, 18089.
- (14) Erbs, W.; Desilvestro, J.; Borgarello, E.; Gratzel, M. *J. Phys. Chem.* **1984**, *88*, 4001.
- (15) Miseki, Y.; Kusama, H.; Sugihara, H.; Sayama, K. *J. Phys. Chem. Lett.* **2010**, *1*, 1196.
- (16) Konda, R.; Ishii, T.; Kato, H.; Kudo, A. *J. Phys. Chem. B* **2004**, *108*, 8992.
- (17) Kato, H.; Hori, M.; Konda, R.; Shimodaira, Y.; Kudo, A. *Chem. Lett.* **2004**, *33*, 1348.
- (18) Clark, S. J.; Segall, M. D.; Pickard, C. J.; Hasnip, P. J.; Probert, M. J.; Refson, K.; Payne, M. C. *Z. Kristallogr. - Cryst. Mater.* **2005**, *220*, 567.
- (19) (a) Buhler, N.; Meier, K.; Reber, J. F. *J. Phys. Chem.* **1984**, *88*, 3261. (b) Kasahara, A.; Nukumizu, K.; Hitoki, G.; Takata, T.; Kondo, J. N.; Hara, M.; Kobayashi, H.; Domen, K. *J. Phys. Chem. A* **2002**, *106*, 6750.
- (20) (a) Kusainova, A. M.; Lightfoot, P.; Zhou, W. Z.; Stefanovich, S. Y.; Mosunov, A. V.; Dolgikh, V. A. *Chem. Mater.* **2001**, *13*, 4731. (b) Kusainova, A. M.; Stefanovich, S. Y.; Irvine, J. T. S.; Lightfoot, P. J. *J. Mater. Chem.* **2002**, *12*, 3413.